SAND2016-3234C

Depressurization and Warpage in Glassy PMDI Foams

Kevin N. Long[a1], Christine C. Roberts[a], Lisa A. Mondy[a], Rekha R. Rao[a]

[a]*Engineering Sciences Center, Sandia National Laboratories, Albuquerque NM USA*
knlong@sandia.gov, ccrober@sandia.gov, lamondy@sandia.gov, rrrao@sandia.gov

Abstract. We investigate how manufacturing conditions result in the warpage of moderate density PMDI polyurethane foam (12-40 lb/ft^3). Previous efforts hypothesized that the manufacturing stresses and viscoelasticity of the matrix were the main drivers of dimensional change in glassy foamed parts. In this work, we now examine the effects of over-pressured CO_2 in the foam microstructure that originates from the simultaneous foaming and curing reactions, the role of density variation, and the associated model characterization. We present experimental measurements of specific components made with realistic manufacturing conditions and their long-term warpage behavior. After the initial manufacturing stresses, gas depressurization appears to be an important mode of deformation, giving the correct time scale of warpage compared to experimental data. Depressurization can be straightforwardly incorporated into our finite element cradle-to-grave framework for chemically blown foams, and we discuss varying levels of model complexity and their associated predicted responses.

Keywords: Coupled Physics Modeling, Bubble Depressurization, Shape Stability, and Mechanical Behavior
PACS: 44, 46, 47, 83

INTRODUCTION

Dimensional change over time can be problematic for PMDI polyurethane foamed components with geometric tolerance requirements. We are working to develop an understanding of the connection between manufacturing conditions and dimensional stability, to one day mitigate it. Several rigid and flexible foams have been examined in the literature in the context of aging and dimensional change [1-4], with a variety of proposed mechanisms: depressurization of excess blowing agent, residual stress and viscoelasticity of the matrix, additional (thermoset) curing, and humidity induced swelling. We are interested in rigid PMDI foams for encapsulation and structural components. These exhibit post-manufacture warpage over times scales of at least a year [1]. Polystyrene foams have also seen dimensional changes over similar time scales [2].

The PMDI foams of interest are glassy at room temperature (T_g >100ºC); thus we anticipate dimensional change due to additional matrix curing to be negligible. Moreover, our experiments maintain a desiccated environment to remove moisture effects. We are left with two viable mechanisms: viscoelasticity and bubble depressurization of the blowing agent. Outside the scope of this paper, we are studying the former, although the time scale of relaxation appears to be long compared to one year. Here, we focus on the depressurization mechanism. We note that effective CO_2 diffusion in polyurethane foams, for the thicknesses of our parts, produce time scales similar to our experimental measurements. We conjecture that spatial variations in density and CO_2 bubble pressurization result in spatially dependent warpage [2]. Our approach differs from the cited literature in two ways: first, we develop a simple micromechanics model that connects density and gauge pressure to the (local) macroscale warpage, and extend this model to a 3D constitutive equation useful for finite element simulation. Second, we control the manufacture and then measure the dimensional change over the course of 200 days of a foam geometry with both thick and thin regions. We compare theory and measurements where possible

A SIMPLE MICROMECHANICS MODEL FOR DEPRESSURIZATION IN FOAMS

We seek a simple means of estimating the extent of warpage possible due to gas depressurization as a function of excess CO_2 pressure, foam density, and matrix phase mechanical properties. The model is based on the idea that excess pressure in the foam bubbles diminishes as the gas phase pressure equilibrates with the surrounding ambient

[1] Sandia National Laboratories is a multi-program laboratory managed and operated by Sandia Corporation, a wholly owned subsidiary of Lockheed Martin Corporation, for the U.S. Department of Energy's National Nuclear Security Administration under contract DE-AC04-94AL85000.

pressure over time. The time scale is set by CO_2 diffusion out of the gas bubbles though the solid matrix and into the surrounding environment. (Note, counter diffusion of air into the bubbles occurs but does not lead to over-pressurization.) Under suitable conditions, this phenomenon is a gas diffusion problem at the component length scale with an effective diffusion coefficient. However, our focus in this work is on the associated mechanical consequences of gas leaving the component. We ignore the transport time scale in this section and estimate the net depressurization warpage subject to three simplifying assumptions: uniform density, uniform excess gas pressure, and statistically isotropic foam microstructure at the macroscale. Later, we will relieve the first two assumptions by recasting this theory in 3D constitutive form. Under these simplifying assumptions, the net depressurization strains are volumetric and the same everywhere in the component. To compute this volume strain response, we idealize the foam microstructure with a spherical representative volume (RV) illustrated in Figure 1(a), and we compute the net volume change between the pressurized and depressurized configurations.

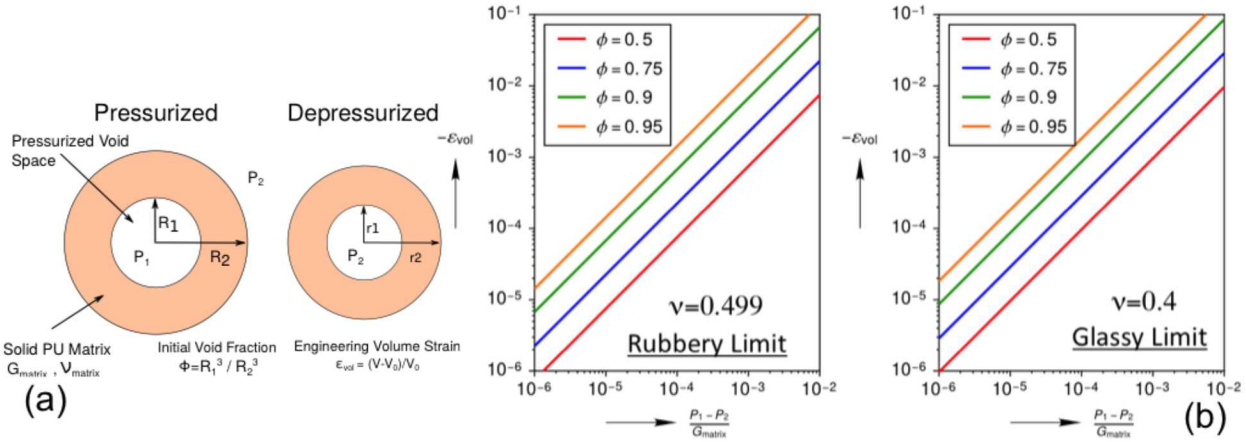

FIGURE 1. (a) Spherical representative volume of the average foam microstructure. The RV illustrates the key model parameters: void volume fraction, matrix phase properties, and initial gauge pressure. (b) Map of the net volume shrinkage due to depressurization for typical rubbery and glassy foams associated with the RV in (a) and its underlying assumptions.

Our depressurization problem is a re-interpretation of the pressurization of an elastic shell that is standard in the literature [5]. The shell deforms in a spherical symmetric manner with a radial displacement field characterize by:

$$u = A_1 + \frac{A_2}{R^3}, \qquad A_1 = \frac{P_2 R_2^3 - P_1 R_1^3}{3K_{matrix}\left(R_1^3 - R_2^3\right)}, \qquad A_2 = \frac{R_1^3 R_2^3 \left(P_2 - P_1\right)}{4G_{matrix}\left(R_1^3 - R_2^3\right)}. \tag{1}$$

Here, K_{matrix} and G_{matrix} are the bulk and shear moduli of the matrix phase. Evaluating the radial displacement field at R_2 and asserting that the deformation is spherically symmetric, one can compute the volume strain associated with full depressurization of this RV:

$$\lambda_R = 1 + \frac{u|_{R_2}}{R_2} = 1 + \left(\frac{4G_{matrix}\left(P_1\phi - P_2\right) - 3\phi\left(P_1 - P_2\right)}{12G_{matrix}K_{matrix}\left(1-\phi\right)} \right), \qquad \varepsilon_{vol} = \log\left(\lambda_R^3\right) \tag{2}$$

We reduce the depressurization response to three dimensionless variables: the ratio of the initial gauge pressure to the shear modulus $(P_1 - P_2)/G_{matrix}$, void volume fraction $\phi = R_1^3 / R_2^3$, and matrix phase Poisson Ratio ν. A map of the net volume strain magnitude due to warpage is provided in Figure 1(b) for the bounding cases of typical rubbery and glassy foams. From the map in Figure 1(b), we make several observations. First, in the small strain limit of the RV, the extent of warpage is directly proportional to the dimensionless gauge pressure for the different foam densities considered. Second, foam density has a significant impact. Low-density foams may warp orders of magnitude more than higher density foams for the same dimensionless gauge pressure. Finally, the effect of the matrix Poisson's ratio is secondary relative to the gauge pressure.

EXTENDING THE MODEL TO A 3D CONSTITUTIVE RELATIONSHIP

We relieve two of the three overly simple assumptions of the previous section by extending the analytic representation of foam depressurization to a 3D macroscale constitutive relationship suitable for finite element

analysis. The present formulation still assumes isotropic behavior at the macroscale. Consider the motion of a foam body that carries material points within it from a reference state, which we will take to be the undeformed state just after manufacture of the component, to the current configuration of the body at a later time. We assume that the gradient with respect to the referential coordinates of the current position (the deformation gradient) may be multiplicatively split into volumetric and isochoric pieces, and we compute the symmetric rate of deformation following standard methodology [5].

$$\mathbf{F} = \mathbf{F}^{iso}\mathbf{F}^{vol}, \qquad \mathbf{D} = \mathbf{D}^{iso} + \mathbf{D}^{vol} \tag{3}$$

Following the previous section, RV depressurization determines only a volume strain response. We therefore further decompose the volumetric portion of the deformation gradient and rate of deformation into thermal, mechanical (stress producing), and depressurization contributions:

$$\mathbf{F}^{vol} = \lambda_\theta \lambda_M \lambda_d \mathbf{1}, \qquad \mathbf{D}^{vol} = \left(\frac{\dot{\lambda}_\theta}{\lambda_\theta} + \frac{\dot{\lambda}_M}{\lambda_M} + \frac{\dot{\lambda}_d}{\lambda_d} \right) \mathbf{1} = \mathbf{D}_\theta^{vol} + \mathbf{D}_M^{vol} + \mathbf{D}_d^{vol}. \tag{4}$$

The key ingredient is the depressurization rate of deformation. Using the RV from the previous section, we compute the derivative of the radial displacement with respect to the gauge pressure, which itself is a function of time t:

$$\dot{\lambda}_d = 1 + \frac{1}{R_2} \frac{d\left(u|_{R_2}\right)}{dP_1} \frac{d\left(P_1 - P_2\right)}{dt}, \qquad \frac{d\left(u|_{R_2}\right)}{dP_1} = \frac{3\phi\left(4G_{matrix} + K_{matrix}\right)R_2}{4G_{matrix}K_{matrix}\left(1-\phi\right)}. \tag{5}$$

The chain rule in equation (5) relies on the assumption that P_2 is constant, which we assign to zero. We recognize that a different choice may be more appropriate. Next, consider an isotropic thermal model with an empirical linear thermal expansion coefficient, α_L, which now allows the calculation of the mechanical rate of deformation:

$$\mathbf{D}_\theta^{vol} = \alpha_L \dot{\theta} \mathbf{1}, \qquad \mathbf{D}_m^{vol} = \mathbf{D} - \mathbf{D}_d^{vol} - \mathbf{D}_\theta^{vol}. \tag{6}$$

We assume the foam behaves macroscopically as an isotropic elastic material with elastic constants derived from average properties of the Weaire-Phelan microstructure rather than from the RV in Figure 1(a) [6]:

$$\dot{\sigma} = 2G_{WF}\,\mathrm{dev}\mathbf{D}_M + K_{WF}\left(\mathrm{tr}\mathbf{D}_M\right)\mathbf{1}, \qquad G_{WF} = 0.113\left(1-\phi\right)E, \qquad K_{WF} = 0.434\left(1-\phi\right)E \tag{7}$$

Here, E is the matrix phase Young's modulus and $\dot{\sigma}$ is the time derivative of the macroscale Cauchy stress, which is not objective, and so we use the Green-Naghdi stress rate in conjunction with equation (7) to satisfy objectivity of the momentum balance (as is standard for a hypoelastic model). We note that the Weaire-Phelan microstructure produces mildly anisotropic elastic constants. Here, we have averaged the [111] and [100] directions. Moreover, these constants apply only to the low relative density limit $\left(1-\phi\right) \sim 0$. Since both thermal expansion and depressurization produce volumetric deformation in this model, all other motion is stress-producing in equation (7). The constitutive model inputs are: $\left\{G_{matrix},\ K_{matrix},\ \alpha_L,\ f_0,\ \left(P_1 - P_2\right)\right\}$. Other elastic constants can be derived from the matrix shear and bulk moduli. The last two quantities vary spatially, and the last varies in time. While the first three may be uniform for the foam, the last two must be initialized and provided to the constitutive model everywhere in the foam component as a function of time if one seeks to capture the time and spatial dependence of the gas depressurization and warpage process. Although future plans are to predict these spatial dependencies using a model for foam blowing and cure, here we discuss initialization based on a model experiment in the next section.

MEASUREMENTS OF WARPAGE IN A TEST GEOMETRY OVER 200 DAYS

Experimental Conditions

A carefully controlled experiment was devised to provide long-term observations of foam shrinkage. Experimental conditions aimed to create a foam part with both thin and thick sections: a staple shaped geometry was chosen as illustrated in Figure 2(b). The mold is primarily aluminum with an acrylic faceplate that allows visualization of the flow path of the material. Foam is injected with the mold in a "U" orientation at its base so that it reacts, expands, and rises symmetrically into the two points. Vents are located at the point tips to allow air to escape as it is displaced. Six calibrated thermocouples (Omega, K-type) and two pressure transducers (Omega, T900) are placed at various locations in the mold flush with the wall (Figure 2(a)) so that the temperature and pressure of the foam is recorded as it reacts exothermically to fill the mold.

A polyurethane foam kit (BKC 44306 PMDI-10, obtained from the National Security Center, Kansas City, Mo) with a free-rise theoretical density of 10 lb/ft^3 is used. This formulation initially consists of separate resin and curative liquids that are mixed and injected into a pre-heated mold that is temperature controlled in a 40°C oven throughout the experiment. Enough material is injected to slightly over-pack the mold to 13 lb/ft^3. The flow path of the foam rising into the mold is videoed through a window in the oven door. Once the foam has finished expanding, the acrylic faceplate is replaced with an aluminum plate and the sample is cured at 120°C for 4 hours per standard procedure. Specimens are then removed from the mold, cooled to room temperature, bolted to a fixture to stand upright, and stored in a dry environment for long periods of time. Periodically the specimen dimensions are measured using a Zyce Coordinate Measurement Machine (CMM) using a 100 mN probe force. This instrument has a calibrated linear accuracy of 5 μm for the 100 mm length of the base of the geometry. Traces along both the female and male portions of the specimen were made at five separate thicknesses. Additionally, an X-ray CT scan was made of the specimens (North Star Imaging) in order to measure their interior density and identify voids.

Results

Triplicate specimens were foamed in the mold with good reproducibility of the temperature and pressure profiles. As expected, the base of the staple, which is reached by foam first and is the thickest part of the geometry, reaches the highest temperatures (90°C peak temperature). A slight temperature rise is also observed at the foam tips (50°C). Gauge pressures were observed up to 14 psig at the mold walls; pressures and temperatures are predicted to be higher internally to the sample. X-ray CT images (Figure 2(c)) identify large bubbles that are primarily located in the two upright arms. A dense skin reaching over 20 pcf is also observed at the mold walls as in the front image. Coalescence and formation of large bubbles has been observed previously in regions of high shear in other experiments. A greater packing fraction for this foam would reduce these defects. Finite element simulations were performed on this geometry from the room temperature state onward using the X-ray CT density. We used the peak measured pressure, ~14 psig, from Figure 2(a), and applied it uniformly to the part though likely the internal initial gauge pressures are much higher and are functions of density. Typical glassy polymer matrix elastic constants were used ($G \sim 1$ GPa, $\nu \sim 0.4$). We simulated a uniform decay of the gauge pressure and fixed the collections of nodes corresponding to the bolts in the experiment. Similar measurements of dimension change at the waist and 80% along the staple tip were extracted. We found that warpage was an order of magnitude or more lower than experiments, likely a result of too simple an initial gauge pressure. We found that predicted warpage was very sensitive to that initial pressure. Qualitatively, the simulations are useful in that they show large regions tend to warp uniformly, but in thin regions, warpage varies spatially. The final warped shapes of the mid section and front are shown in Figure 2(d).

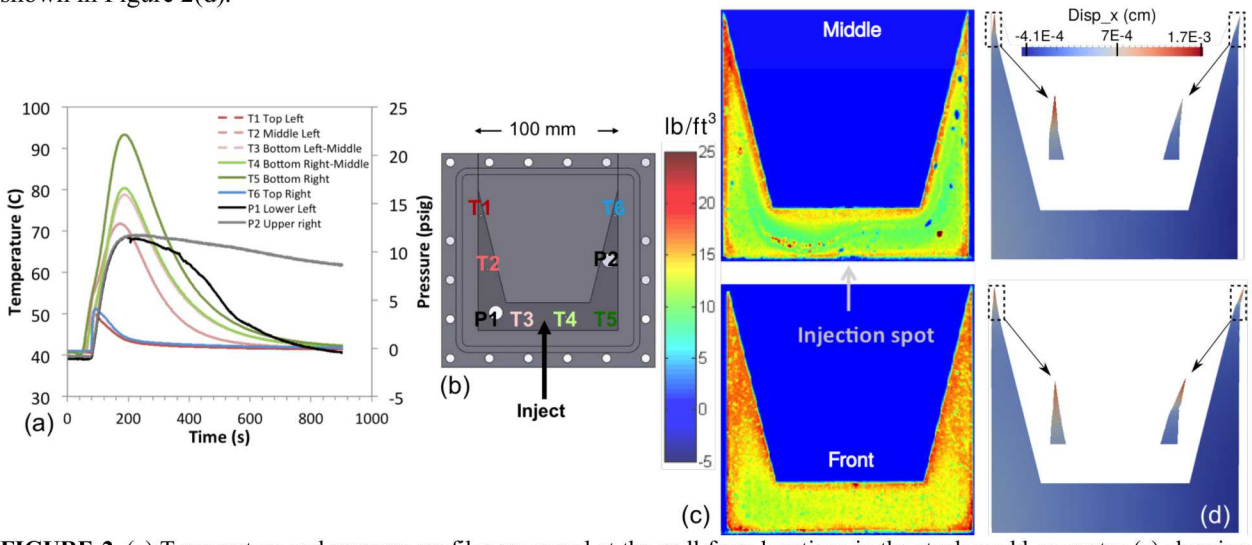

FIGURE 2. (a) Temperature and pressure profiles measured at the wall from locations in the staple mold geometry (a) showing locations of thermocouples (T), pressure transducers (P), and the injection port. Time is measured from the mixing time of the two components. (c) False color X-ray CT image of the density of a specimen halfway through the middle of the sample (into the page), showing many large bubbles in the arms and a high density skin near the walls. (d) Corresponding FEA showing the fully depressurized warped state along the middle and front slices. Note the distinct warpage at the tips between the two slices.

The dimensional change of a foamed specimen is measured at both the base and 80% of the distance to the tips. The dimensional change at each location is displayed in Figure 3 with respect to the aluminum mold width at the cure temperature of 120ºC. At the base, a large initial shrinkage of about 0.6% is observed at short times that is attributable to the thermal contraction of the sample. Then, over approximately 14 days, a slow contraction is observed that adds an additional 0.1% shrinkage. This contraction diminishes over time until it is approximately equal to the error in the measurement. The width of the staple at the arms of the specimen follow an unpredictable, unsteady movement. This movement could be due to the anomalous large bubbles contained within the arm or some other unknown factor.

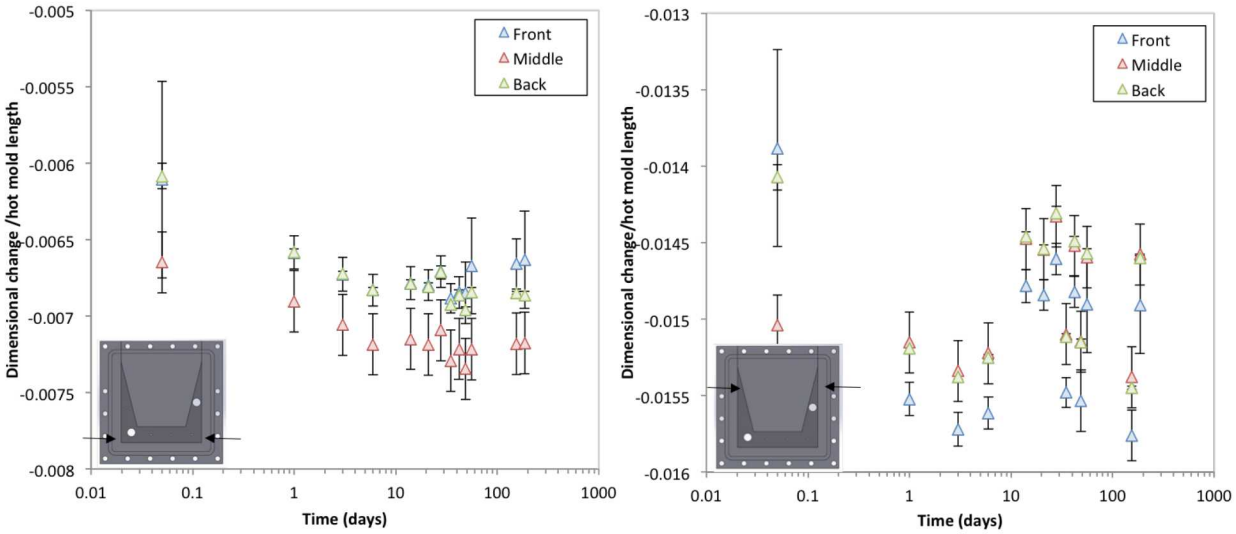

FIGURE 3. Staple width dimensional change normalized by the predicted mold width at the curing temperature (120 oC) for (left) the base of the staple and (right) 80% up the staple arms. Front, middle, and back refer to the location of the trace in the depth of the mold (into the page as pictured)

CONCLUSIONS

We have measured the dimensional change of a chemically blown PMDI 13 lb/ft^3 foam over the course of 200 days, and these measurements show that, despite large defects within the foam from processing, overall shrinkage is more uniform in thick regions than in thin regions. Accompanying FEA simulations using a constitutive model based on a simple micromechanics model of foam depressurization corroborates this finding. We note that under uniform density/gauge pressure conditions, the model is analytic, and it shows a direct trade offs between gauge pressure, foam porosity, and volume change due to depressurization.

REFERENCES

1. R. D. Gilbertson, B. M. Patterson, and Z. Smith. Accelerated aging of BKC44306-10 rigid polyurethane foam: FT-IR spectroscopy, dimensional analysis, and micro computed tomography. *LA-UR-14-20007*, Los Alamos National Laboratory, January 2014.
2. T. Fen-Chong, E. Herve, and A. Zaoui. Micromechanical modeling of intracellular pressure-induced viscoelastic shrinkage of foams: application to expanded polystyrene. *European Journal of Mechanics, A/Solids*, 18, 1999.
3. M. Rampf, O. Speck, T. Speck, and R. H. Luchsinger. Structural and mechanical properties of flexible polyurethane foams cured under pressure. *Journal of Cellular Plastics*, 48:53–69, 2011.
4. C. T. Yang, K. L. Lee, and S. T. Lee. Dimensional stability of LDPE foams: Modeling and experiments. *Journal of Cellular Plastics*, 38:113– 128, 2002
5. I. S. Sokolnikoff. *Mathematical Theory of Elasticity*. McGraw-Hill. 2nd Ed. 1956.
6. J. F. Sadoc and N. Rivier. *Foams and Emulsions*. Nato Science Series E: Applied Sciences Vol. 354. Springer, 1999.